



Pallido-putaminal connectivity predicts outcomes of deep brain stimulation for cervical dystonia

✉ Ashley L. B. Raghu,¹ John Eraifej,^{1,2} Nagaraja Sarangmat,³ John Stein,⁴ James J. FitzGerald,^{1,2} Stephen Payne,⁵ Tipu Z. Aziz^{1,2} and Alexander L. Green^{1,2}

Cervical dystonia is a non-degenerative movement disorder characterized by dysfunction of both motor and sensory cortico-basal ganglia networks. Deep brain stimulation targeted to the internal pallidum is an established treatment, but its specific mechanisms remain elusive, and response to therapy is highly variable. Modulation of key dysfunctional networks via axonal connections is likely important.

Fifteen patients underwent preoperative diffusion-MRI acquisitions and then progressed to bilateral deep brain stimulation targeting the posterior internal pallidum. Severity of disease was assessed preoperatively and later at follow-up. Scans were used to generate tractography-derived connectivity estimates between the bilateral regions of stimulation and relevant structures.

Connectivity to the putamen correlated with clinical improvement, and a series of cortical connectivity-based putaminal parcellations identified the primary motor putamen as the key node ($r = 0.70$, $P = 0.004$). A regression model with this connectivity and electrode coordinates explained 68% of the variance in outcomes ($r = 0.83$, $P = 0.001$), with both as significant explanatory variables.

We conclude that modulation of the primary motor putamen–posterior internal pallidum limb of the cortico-basal ganglia loop is characteristic of successful deep brain stimulation treatment of cervical dystonia. Preoperative diffusion imaging contains additional information that predicts outcomes, implying utility for patient selection and/or individualized targeting.

- 1 Oxford Functional Neurosurgery, Nuffield Department of Surgical Sciences, University of Oxford, Oxford, UK
- 2 Department of Neurosurgery, John Radcliffe Hospital, Oxford University NHS Foundation Trust, Oxford, UK
- 3 Department of Neurology, John Radcliffe Hospital, Oxford University NHS Foundation Trust, Oxford, UK
- 4 Department of Physiology, Anatomy and Genetics, University of Oxford, Oxford, UK
- 5 Institute of Biomedical Engineering, Department of Engineering, University of Oxford, Oxford, UK

Correspondence to: Ashley Raghu
Pembroke College, St Aldates, Oxford OX1 1DW, UK
E-mail ashley.raghu@pmb.ox.ac.uk

Keywords: spasmodic torticollis; globus pallidus interna; putamen; tractography; motor cortex

Abbreviations: GPi = globus pallidus interna; HF-DBS = high-frequency deep brain stimulation; M1 = primary motor cortex; STN = subthalamic nucleus; TWSTRS = Toronto Western Spasmodic Torticollis Rating Scale

Received April 01, 2021. Revised June 14, 2021. Accepted July 01, 2021. Advance access publication July 22, 2021

© The Author(s) (2021). Published by Oxford University Press on behalf of the Guarantors of Brain.

This is an Open Access article distributed under the terms of the Creative Commons Attribution-NonCommercial License (<https://creativecommons.org/licenses/by-nc/4.0/>), which permits non-commercial re-use, distribution, and reproduction in any medium, provided the original work is properly cited. For commercial re-use, please contact journals.permissions@oup.com

Introduction

Surgical targeting of the pallidum for the treatment of dystonia emerged from clinical observations in Parkinson's disease, namely improvement in dystonic features following pallidotomy.¹ Observational and interventional data have subsequently indicated substantial benefit from stereotactic treatment of the pallidum in dystonia, and high-frequency (HF) deep brain stimulation (DBS) to the posterior region of the internal pallidum (globus pallidus interna, GPi) is established as the treatment of choice for medically refractory cervical dystonia.² However, clinical improvement can be highly variable, the reasons for which are not understood.

Focal dystonias, such as cervical dystonia, are characterized as sensorimotor network disorders, involving anatomical structures including the pallidum, striatum, primary sensorimotor cortex, thalamus, and cerebellum. They feature abnormal low frequency coherence, reduced excitability of inhibitory systems, and dysfunctional plasticity associated with abnormal neural topography.^{3–5} Network normalization is thought to be the meta-mechanism of effective GPi HF-DBS,⁶ possibly achieved by suppressing abnormally enhanced synchronized low frequency oscillatory activity within the motor cortico-basal ganglia network, with a reduction of both pallido-cortical coherence and excessive motor cortex plasticity.

The GPi is the main output node of the basal ganglia to the thalamus, and receives input primarily from the striatum (putamen for the motor-sensory circuit), but also the subthalamic nucleus (STN). Neuromodulation of one or more of these structures, via their direct connections, is plausibly an important determinant of the magnitude of clinical benefit derived from GPi HF-DBS. We used diffusion-weighted MRI tractography to derive connectivity estimates between DBS leads and these three nuclei to explore possible relationships with clinical improvement.

Materials and methods

Patients

Nineteen patients [age at surgery 54.9 (mean standard deviation, SD) years, eight male] with severe, medically refractory isolated cervical dystonia, or cervical dystonia accompanied by dystonia in additional body parts, underwent implantation of bilateral electrodes (Table 1) in the GPi, undergoing surgery as described elsewhere,⁷ at the John Radcliffe Hospital. All patients underwent assessment by a consultant neurologist, neurosurgeon and neuropsychologist, all with expertise in movement disorders, before being offered surgical treatment. Neuroimaging was performed under general anaesthetic, as pathological head movement otherwise typically precludes an adequate acquisition.

Clinical rating

The patient's pre- and postoperative [12 months (range 6–18 months)] clinical state was assessed using the Toronto Western Spasmodic Torticollis Rating Scale of severity (TWSTRS-s; score/35) by a neuromodulation movement disorder specialist nurse or a consultant functional neurosurgeon.

Diffusion imaging acquisition and preprocessing

In 15 patients, preoperative MRI was performed on a 1.5 T Phillips Achieva using a modified spin-echo sequence with SENSE parallel imaging. In-plane resolution was 1.818 by 1.818 mm², and 64 2-mm thick slices were acquired in an interleaved fashion. Diffusion

weighting ($b = 1200 \text{ s/mm}^2$) was applied along 32 non-colinear gradient directions, with one non-diffusion-weighted volume ($b = 0$). Correction for distortions and subject movement was carried out using the FMRIB Software Library (FSL; Oxford, UK). The susceptibility-induced off-resonance field was estimated using *topup*. Instead of using two $b = 0$ spin-echo EPI with opposing phase-encoding (PE) direction, the field was estimated from a $b = 0$ volume and a structural T₂-weighted scan, without any distortions.

Four additional patients underwent a higher angular resolution acquisition. Preoperative MRI was performed on a 3 T Siemens TrioTim using a modified spin-echo sequence with parallel imaging. In-plane resolution was $2 \times 2 \text{ mm}^2$, and 64 2-mm thick slices were acquired in an interleaved fashion. Diffusion weighting ($b = 1500 \text{ s/mm}^2$) was applied along 60 gradient directions that were chosen to sample the sphere evenly by minimization of Coulomb forces, with four non-diffusion-weighted volumes ($b = 0$). This was performed twice, with opposing PE direction (128 volumes in total). The susceptibility-induced off-resonance field was estimated using *topup*, with two $b = 0$ spin-echo EPI with opposing PE direction.

In all 19 patients, motion and eddy currents were corrected for using eddy, with outlier detection and replacement. Single shell ball and stick modelling of local diffusion parameters was carried out using BEDPOSTX, with up to three crossing fibres per voxel.

Deep brain stimulation

Patients were programmed to maximize improvements in dystonia. Initially, imaging was reviewed to select an appropriate contact for stimulation, usually the second deepest contact. High frequency stimulation was introduced, and patients typically discharged with two or three programmes for use at patient preference, and the ability to titrate amplitude within an allowed window. For patients with a poor response, alternative contacts were explored, usually at 3-month review.

Termination masks

FIRST, a Bayesian model-based segmentation/registration tool in FSL, was applied to same session T₁-weighted MRI scans (1 mm isotropic) to extract thalamic and putaminal masks for each patient, with boundary voxels excluded. The Montreal Neurological Institute (MNI) structural atlas was used to generate masks of the frontal and parietal cortices. The Harvard–Oxford cortical atlas was used to generate masks of the superior frontal gyrus (cropped to the caudal portion, SFGc), middle frontal gyrus (MFG), inferior frontal gyrus pars opercularis (IFGpo), primary motor cortex (M1), and supplementary motor area (SMA), which were then registered to T₁-weighted MRI scans using FLIRT and FNIRT. SFGc and SMA were combined to approximate the dorsal premotor cortex (PMd), while the MFG and IFGpo were combined to approximate the ventral premotor cortex (PMv).

Tractography and parcellation

Probabilistic tractography was carried out using PROBTRACX, with modified Euler streaming and distance correction. A bidirectional arrow (\longleftrightarrow) is used hereafter to reference connectivity between two regions. Postoperative CT images were registered to MRI using FLIRT. Lead contacts were identified based on CT artefacts and array dimensions. Stimulation parameters at follow-up were reviewed and the most-used cathode contact identified (in patient M, an average between two contacts was taken, as two programs with different cathodes were equally used). For each lead, a 3 mm radius sphere around this contact, was used as a tractography seed to thalamus, putamen and STN. Tracts were visualized for

Table 1 Clinical characteristics

Patient	Age at surgery, sex	Aetiology	Age of onset	Body distribution	Predominant cervical dystonia features	Sensory trick	Associated features	Preoperative TWSTRS severity	TWSTRS severity improvement	TWSTRS severity improvement (%)	Follow-up/ months
A	61, F	Idiopathic sporadic ^a	Early adulthood	Focal cervical	Phasic laterocollis	No	Isolated dystonia	22	5	23	18
B	45, F	Idiopathic sporadic	Late adulthood	Focal cervical	Phasic torticollis	Yes	Isolated dystonia	19	4	21	12
C	46, F	Idiopathic familial, AD	Adolescence	Focal cervical	Phasic, laterocollis, torticollis	Yes	Isolated dystonia	17	13	76	13
D	54, F	Idiopathic sporadic	Early adulthood	Segmental cervical + orofacial	Tonic anterocollis, torticollis	Yes	Isolated dystonia	13	–3	–23	10
E	44, F	Idiopathic sporadic	Early adulthood	Focal cervical	Tonic torticollis, laterocollis	Yes	Isolated dystonia	16	4	25	11
F	47, F	Idiopathic sporadic	Late adulthood	Focal cervical	Phasic torticollis, laterocollis	Yes	Isolated dystonia	14	1	7	12
G	46, F	Idiopathic sporadic	Early adulthood	Focal cervical	Tonic laterocollis, torticollis	Yes	Isolated dystonia	17	5	29	12
H	60, M	Idiopathic sporadic	Late adulthood	Focal cervical	Phasic torticollis, laterocollis	Yes	Isolated dystonia	22	13	59	12
I	66, M	Idiopathic sporadic	Late adulthood	Focal cervical	Tonic anterocollis	Yes	Isolated dystonia	18	–1	–6	12
J	72, F	Idiopathic sporadic	Late adulthood	Segmental cervical + orofacial + blepharospasm	Phasic anterocollis	Yes	Isolated dystonia	26	16	62	12
K	67, M	Idiopathic sporadic	Late adulthood	Focal cervical	Phasic torticollis, retrocollis	Yes	Isolated dystonia	20	4	20	12
L	49, M	Idiopathic sporadic	Late adulthood	Segmental cervical + shoulder/brachial	Tonic laterocollis, torticollis	Yes	Isolated dystonia	16	4	25	6
M	54, F	Idiopathic sporadic	Late adulthood	Segmental cervical + orofacial + blepharospasm	Tonic, anterocollis, torticollis	Yes	Isolated dystonia	18	12	67	7
N	43, M	? Acquired Toxic ^b	Early adulthood	Segmental cervical + brachial	Tonic torticollis, laterocollis	No	Isolated dystonia	29	11	38	12
O	61, M	Idiopathic sporadic	Late adulthood	Segmental cervical + orofacial	Phasic anterocollis, torticollis, laterocollis	Yes	Isolated dystonia	19	11	58	13
P	61, F	Idiopathic sporadic	Early adulthood	Focal cervical	Tonic laterocollis, torticollis	Yes	Isolated dystonia	24	8	33	12
Q	50, F	Idiopathic sporadic	Early adulthood	Focal cervical	Tonic laterocollis, torticollis	No	Isolated dystonia	23	16	70	13
R	57, M	Idiopathic sporadic	Late adulthood	Focal cervical	Phasic torticollis, laterocollis	Yes	Isolated dystonia	25	12	52	17
S	45, F	Idiopathic sporadic	Early adulthood	Focal cervical	Tonic laterocollis, torticollis	Yes	Isolated dystonia	19	–10	–53	13

AD = autosomal dominant; F = female; M = male. Adolescence, 13–20; early adulthood, 21–40; late adulthood, >40 years.

^aAssumed as patient adopted, not knowing birth parents.^bHistory of intravenous drug use (amphetamines) and alcoholism.

anatomic plausibility. Connectivity-based hard parcellation of the putamen was carried out using the ‘find the biggest’ algorithm in FSL,⁸ first with the frontal and parietal cortex, then second with M1, PMd and PMv as cortical classifiers. The same tractography was carried out to these putaminal parcellations.

Statistical analysis

For each of the streamlines from the cathode generated by PROBTRACX, we counted the number of seeds that reached each region and normalized these by size of the termination mask. Those counts were summed over left and right for each patient, and explored for linear relationships with clinical TWSTRS-s improvement by calculating Pearson, Spearman’s Rho and Kendall’s Tau correlation coefficients (two-tailed).

Coordinate-connectivity relationship

Disambiguating the relative contributions of individual’s electrode locations and diffusion parameters to the observed improvement-tractography correlation is crucial to its interpretation. To assess this, the anterior commissure–posterior commissure (AC-PC) coordinates were measured (neuroinspire™, Renishaw, UK), and the correlation with clinical improvement calculated using the methodology of Schönecker et al.⁹ Then, a forward multiple regression was performed with coordinates and HF-DBS→M1 putamen connectivity as explanatory variables. In addition, the DBS tractography to the putamen was repeated in a common connectome, thereby removing individual differences in diffusion parameters as a variable. To achieve this, one patient’s diffusion scan and all electrode locations were registered to the MNI template, and tractography performed in this common space. This was then repeated with a second diffusion scan for confirmation.

While a therapeutic sweet spot is recognized,¹⁰ these are distributions that many patients do not conform to. This strongly supports an individualized approach. To probe whether these results might have use in augmenting targeting, and demonstrate how this could be done, an additional four patients were analysed. Preoperative 3 T 1 mm isotropic T₁-weighted magnetization prepared-rapid acquisition gradient echo (MP-RAGE) gave adequate spatial contrast to confidently demarcate the GPi. Individualized M1 putamen connectivity density maps of each GPi were generated, the region of highest connectivity (hotspot) was identified and proximity to the lead assessed.

Standard protocol approvals, registrations and patient consents

Research approval was obtained by a local ethics committee (NRES SOUTH CENTRAL OXFORD A 08/H0604/58). Patient consent was obtained according to the Declaration of Helsinki.

Data availability

We are happy to make available, on request by clinicians or researchers, any and all data relating to this study that we are able to, within the bounds of our formal ethics and what otherwise may be considered ethically appropriate.

Results

Patient demographics

All 19 patients were successfully implanted with DBS electrodes bilaterally (Fig. 1), and received bilateral HF (125–130 Hz) DBS. Sixteen patients showed improvement in severity of disease at follow-up (Table 1).

Deep brain stimulation connectivity with motor putamen predicts outcomes

In the 1.5-T dataset, a significant positive correlation was observed between HF-DBS→putamen connectivity and clinical improvement (Fig. 2A; $r_p = 0.56$, $P = 0.029$, $r_s = 0.59$, $P = 0.022$). No significant correlation was observed between either HF-DBS→STN or HF-DBS→thalamus and clinical improvement. To examine whether the HF-DBS→putamen relationship was driven by motor or sensory connectivity, a putamen parcellation was performed (similar to Tziortzi et al.¹¹) based on connectivity to frontal (i.e. motor) and parietal (i.e. sensory) cortices (Fig. 2B). A significant positive correlation was observed between HF-DBS→frontal putamen connectivity and clinical improvement ($r_p = 0.58$, $P = 0.023$, $r_s = 0.57$, $P = 0.028$). No significant correlation was observed between HF-DBS→parietal putamen connectivity and clinical improvement. To further characterize the HF-DBS→putamen relationship, a second parcellation was performed to reveal the motor topography (Fig. 2C). No significant correlations were observed between HF-DBS→PMv/PMd putamen and clinical improvement. A significant positive correlation was observed between HF-DBS→M1 putamen connectivity and clinical improvement ($r_p = 0.70$, $P = 0.004$, $r_s = 0.65$, $P = 0.009$). This result was analysed for robustness: it remained significant after substituting ‘%’ for ‘absolute’ TWSTRS-s improvement ($r_p = 0.64$, $P = 0.010$, $r_s = 0.66$, $P = 0.008$), and remained significant after control capping improvement at zero (absolute: $r_p = 0.68$, $P = 0.005$, $r_s = 0.65$, $P = 0.009$, %: $r_p = 0.63$, $P = 0.013$, $r_s = 0.66$, $P = 0.008$).

Connectivity and coordinates are not equivalent

AC-PC coordinates alone explained 44% of the variance in clinical improvement ($r = -0.66$, $P = 0.007$; Supplementary Fig. 1A), but was not significantly correlated with HF-DBS→M1 putamen connectivity ($r = -0.36$, $P = 0.18$; Supplementary Fig. 1B). A forward regression model [$F(2,12) = 12.8$, $P = 0.001$, $r = 0.83$, $r^2 = 0.68$], found both coordinates ($P = 0.02$) and HF-DBS→M1 putamen connectivity ($P = 0.01$) as significant explanatory variables, with the latter entering first as the best fitting variable. The positive correlation of HF-DBS→putamen connectivity with improvement disappeared when tractography was performed with common diffusion parameters ($r_p = -0.30$), and confirmed in a second connectome. In the 3-T dataset, clear variation in the GPi topology of M1 putamen connectivity was observed between patients (see Fig. 3A for examples). Stimulation in the middle/posterior GPi, hot spot coverage, and high connectivity were consistent with clinical benefit (Fig. 3).

Discussion

We hypothesized that the structural connectivity between the GPi and one or more of the subcortical nuclei with which it is directly connected might be an important mediator of the clinical effects of DBS in cervical dystonia. Examining this question using structural connectivity estimates from diffusion-weighted MRI probabilistic tractography, we found a positive correlation between HF-DBS→putamen connectivity and clinical improvement. We then performed two sequential connectivity-based parcellations of the putamen to characterize the region of putamen crucial to this relationship. This revealed that motor putamen, in particular M1 (middle) putamen, was the essential node of HF-DBS connectivity that explained variance in clinical outcomes. The posterior region of the GPi is also characterized as ‘M1’ based on pallido-thalamo-cortical connectivity, is the most common site of active therapeutic contact in the surgical treatment of dystonia,¹² and is the site of

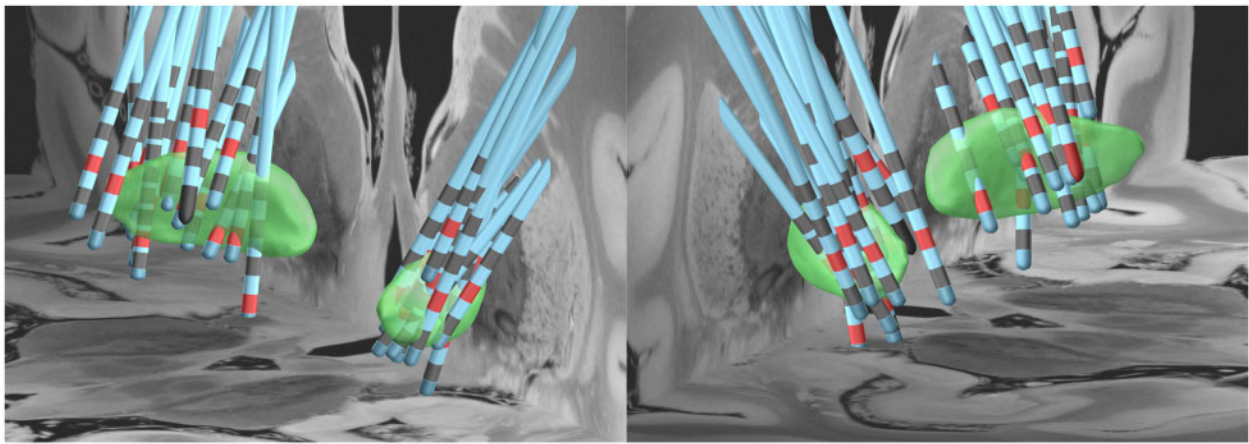


Figure 1 Deep brain stimulation implants. Rendering of electrode location estimates (Patients A–O) in bilateral GPI using LeadDBS.³¹ Red = active cathode.

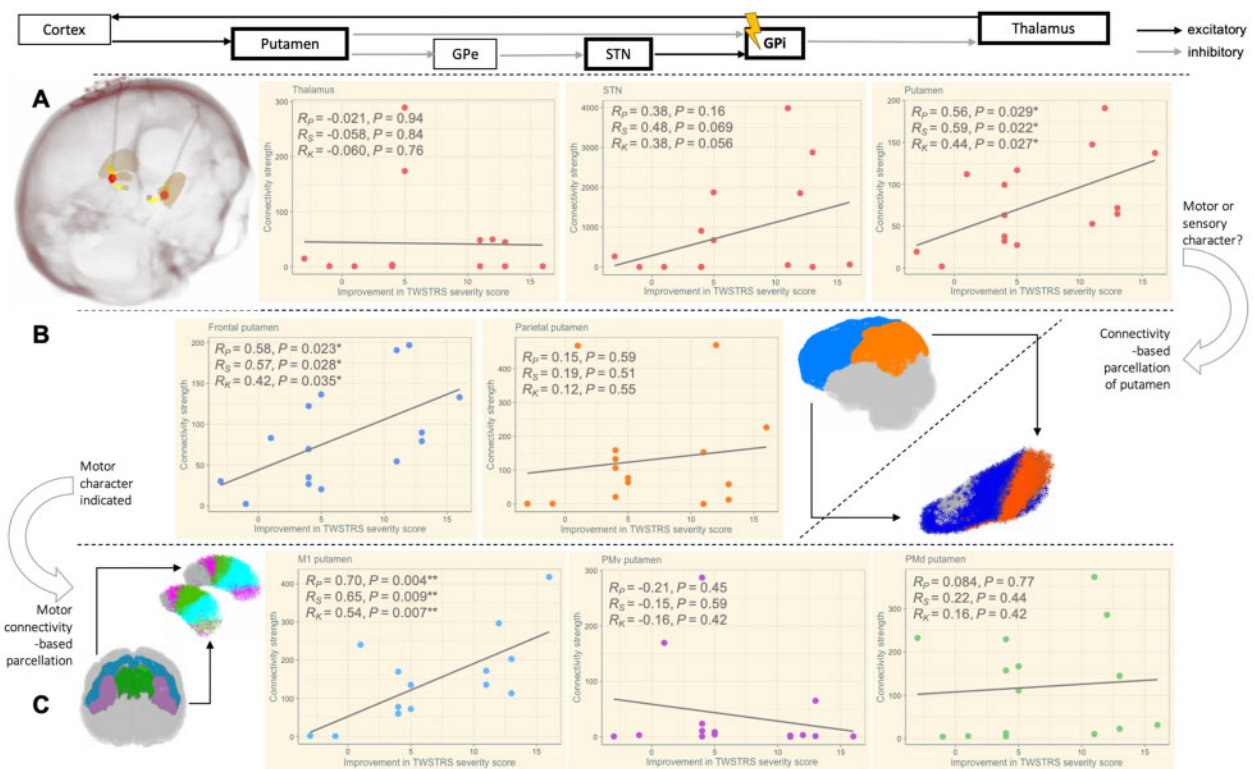


Figure 2 Tractography. Top: Diagram of cortico-basal ganglia-thalamo-cortical loop. (A) Left: 3D fused MR-CT (red) with stimulation (red) and streamlines (yellow) to putamen and STN in 3D view. Right: Initial tractography to STN and putamen with correlation between normalized streamlines and clinical improvement. (B) Right: Frontal and parietal cortical classifiers with example of hard parcellation of the putamen, dividing into regions with high motor and high sensory input. Left: Tractography to frontal and parietal putaminal parcels with correlation between normalized streamlines and clinical improvement. (C) Left: Motor cortical classifiers with bilateral example of hard parcellation of putamina, dividing into regions with high primary motor (M1), high dorsal premotor (PMd) and high ventral premotor (PMv) connectivity. Right: Tractography to M1, PMd and PMv putaminal parcels with correlation between normalized streamlines and clinical improvement. R_p = Pearson's; R_s = Spearman's; R_K = Kendall's coefficients.

local peak theta power: a putative physiomechanical marker for cervical dystonia.¹⁰ Together with our findings, these neuroimaging results point to intervention in the M1-striato-pallido-thalamo-M1 loop as being mechanistically important in relief of dystonia via HF-DBS.

Limitations of our study are found in the data and analysis. While TWSTRS-s ratings were blind to corresponding connectivity

values, they were not blinded to pre- or postoperative status. We expect any bias would be systematic, and therefore not consequential for our conclusions, which rely on correlational analysis. Supplementary analyses indicate triviality of, or no bias (Supplementary Fig. 2). The resolution of the diffusion data is at the lower end suitable to perform our analyses. Replication in an

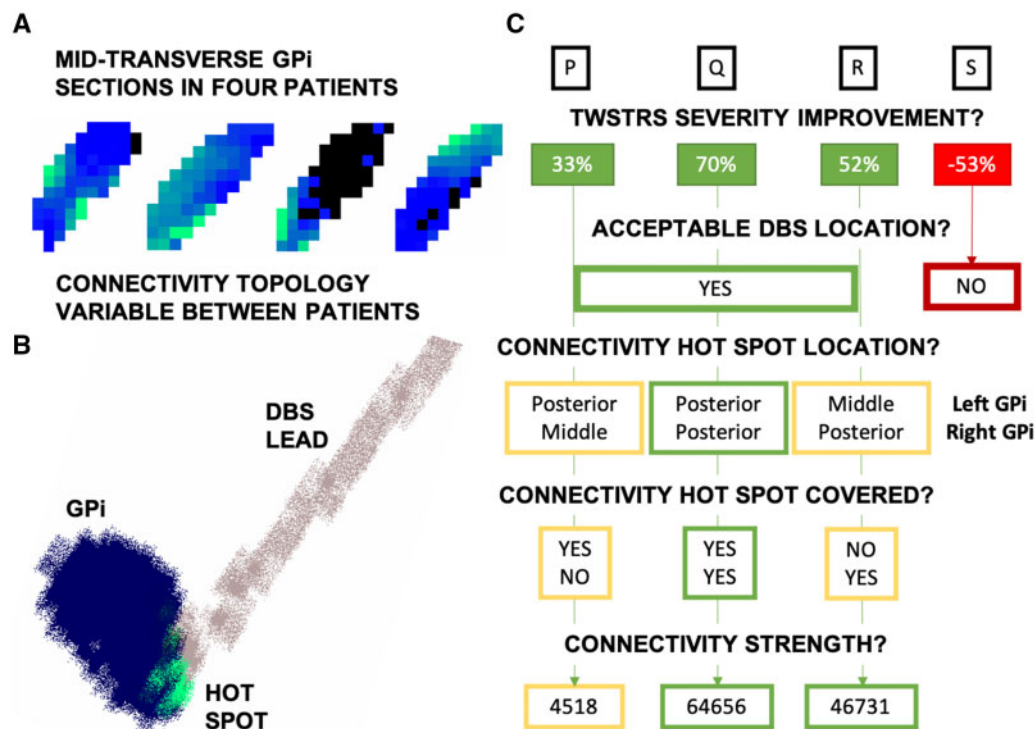


Figure 3 Targeting assessment. Exploration of GPI connectivity in the 3-T cohort as a possible strategy to individualize DBS targeting. (A) Example GPI maps of M1 putamen connectivity density (green = high, blue = low, black = none) demonstrating spatial between patient differences, presenting a putative substrate for individualized targeting. (B) Example rendering (FSLeves) of a DBS lead penetrating a connectivity hotspot (Patient Q). (C) 3-T cohort outcomes rationalized through both electrode location and connectivity, demonstrates congruency with 1.5-T cohort results. Patient S scheduled for lead revision, but delayed due to pandemic. Hotspot is spatial peak M1-putamino-pallidal connectivity. Connectivity strength given as streamlines.

additional cohort is required to confirm our results, and would ideally be carried out at higher resolution. Finally, we used a standardized tractography seed instead of seeding an estimated field of 'activation' for each patient. In short, lack of a validated bipolar-DBS model and changes in both impedance and applied voltage over long-term follow-up created uncertainty, which we felt favoured an identical tractography experiment in every patient.

The putamen is among the most common lesion sites in secondary cervical dystonia,⁶ and is pathologically altered in primary dystonia. Putamen fractional anisotropy is higher in cervical dystonia,¹³ and functional MRI data indicate that putamen somatic topography is disorganized and dedifferentiated in focal hand dystonia.¹⁴ In focal hand dystonia, functional MRI data also indicate decreased activation in the posterior putamen (contralateral to dystonic periphery), but with increased connectivity to primary sensorimotor cortex and increased connectivity of the anterior putamen with premotor cortex.¹⁵ In cervical dystonia, resting state functional MRI has indicated enhanced functional connectivity between anterior putamen and the sensorimotor network.¹⁶ Interrogating the local neurophysiology of GPI HF-DBS in Parkinson's disease with oculomotor neurometry experiments, a pallido-putaminal process of action is considered most likely.¹⁷

Although the sensory component of dystonia pathophysiology is well recognized,^{3,18} abnormal motor cortex, particularly M1, is similarly well established. Reduced excitability of inhibitory circuits in M1 has been demonstrated with TMS,¹⁹ a finding that is supported by GABA-PET studies.²⁰ Increased M1 plasticity is observed in cervical dystonia; a feature that distinguishes these patients from non-manifesting DYT1 carriers.²¹ Indeed, abnormal motor cortex associative plasticity is a core, replicable finding in dystonia,⁴ distinguishing it from psychogenic dystonia,²² with

both long-term potentiation- and long-term depression-like plasticity abnormal with respect to both gain and spatial organization.²³ In addition, the relationship between PMd and M1 is abnormal in both cervical dystonia and focal hand dystonia.²⁴

This advocates a role for both putamen and M1 in the mechanism of GPI DBS in cervical dystonia. Despite clear implication of sensory cortex in cervical dystonia, therapeutic GPI DBS does not correct sensory abnormalities, consistent with sensory systems not mediating motor improvements.²⁵ Low frequency coherence within the basal ganglia-cortical network is a putative signature of dystonia; this coherence between motor cortex and GPI is suppressed by HF-DBS,⁵ a finding also observed in cervical dystonia following a geste antagoniste.²⁶ Furthermore, GPI low frequency DBS evokes potentials in M1, and modulates motor cortex excitability and plasticity.²⁷ There is a reversible reduction in motor cortex excitability with HF-DBS off.²⁸ With HF-DBS on, excitatory motor cortex plasticity is abolished and shifted to cortical inhibition.²⁹ In addition, DBS normalizes increased M1 low frequency oscillations, and their interhemispheric coherence, as well as decreasing M1 activation.³⁰ Taken together, a physiological model of GPI DBS reducing thalamocortical inhibition remains coherent. Our interpretation of our results is that this is achieved via disruption of GABA-ergic inhibitory signalling from the region of putamen receiving dominant input from M1, to the posterior ('M1') GPI. We suggest that the result of this would be increased inhibitory output of the posterior GPI to thalamus, and decreased thalamocortical (M1) signalling. This would manifest electrophysiologically as desynchronization of low frequency coherence in the M1-basal ganglia loop that is observed.

Clearly electrode implant location matters, and surgically this will vary among patients. While this does account for much

statistical variance in clinical outcomes, much remains unexplained, including examples where a primary or secondary anterior/middle GPi lead can be so beneficial. The assumption that pallidal topographic anatomy is essentially the same among cervical dystonia patients may not be justified, warranting an individualized approach. We demonstrated that specific diffusion parameters encode outcome-predictive information additional to that offered by coordinates. Similarly, our results indicated that putamen-GPi tractography patterns do not define a common anatomic region well and that, at least in cervical dystonia, individual differences are substantial. This was confirmed with the 3-T GPi mapping (Fig. 3A). Therefore, this study provides a platform where an individualized surgical approach can be pursued using pre-operative diffusion MRI, with connectivity 'hot spots' as a target modifier. Initial DBS programming could be guided in the same way.

Outside of an 'optimized' DBS location, strength of connectivity from the relevant target and within the dysfunctional network is a prime putative explanatory factor for variance in outcomes. We suppose that total network dysfunction in cervical dystonia is both common and heterogenous. Supporting this, lesions (inevitably leading to loss of connectivity) of numerous nodes can produce the same clinical picture.⁶ Patients with strong connectivity within the M1-putamen-GPi limb of the network may have more potential to benefit from HF-GPi DBS, whereas others may be better treated with STN DBS or other treatments.

In conclusion, although both motor and sensory dysfunction are recognized in cervical dystonia, our study supports a theory of motor-striato-pallidal connectivity, not sensory circuits, as a crucial factor in efficacious DBS.

Acknowledgements

We would like to thank our outstanding and dedicated neuromodulation nurses, in particular Beth and Claire, as well the rest of the movement disorder team, in particular neurologist Marko Bogdanovic. We would also like to express gratitude for the crucial assistance that Jesper Andersson (FMRIB, Oxford) provided with respect to applying his diffusion-MRI preprocessing software to our data, as well as providing consultation on tractography. Last, we would like to thank Trevor Cox (Medical Statistics, Liverpool) for providing consultation on statistics.

Funding

No funding was received towards this work.

Competing interests

J.J.F. receives consultancy fees from Medtronic, Abbott Laboratories and Renishaw, and research grant support from Abbott Laboratories. T.Z.A. has received travel grants from Medtronic, Abbott Laboratories and Boston Scientific. A.L.G. reports he is on Abbott Laboratories' movement disorder executive advisory board, and is faculty for their SCS and DRGS neuromodulation courses, for which he receives personal fees. He is also a data monitoring safety board committee member for a Herantis Pharma trial for PDGF in PD, and also does consultancy with InBrain as an executive advisor.

Supplementary material

Supplementary material is available at *Brain* online.

References

1. Laitinen LV, Bergenheim AT, Hariz MI. Leksell's posteroventral pallidotomy in the treatment of Parkinson's disease. *J Neurosurg.* 1992;76(1):53–61.
2. Albanese A, Asmus F, Bhatia KP, et al. EFNS guidelines on diagnosis and treatment of primary dystonias: EFNS dystonia guidelines. *Eur J Neurol.* 2011;18(1):5–18.
3. Byl NN, Merzenich MM, Jenkins WM. A primate genesis model of focal dystonia and repetitive strain injury: I. Learning-induced dedifferentiation of the representation of the hand in the primary somatosensory cortex in adult monkeys. *Neurology.* 1996;47(2):508–520.
4. Quartarone A, Bagnato S, Rizzo V, et al. Abnormal associative plasticity of the human motor cortex in writer's cramp. *Brain.* 2003;126(Pt 12):2586–2596.
5. Barow E, Neumann W-J, Brücke C, et al. Deep brain stimulation suppresses pallidal low frequency activity in patients with phasic dystonic movements. *Brain.* 2014;137(Pt 11):3012–3024.
6. Corp DT, Joutsa J, Darby RR, et al. Network localization of cervical dystonia based on causal brain lesions. *Brain.* 2019;142(Pt 6):1660–1674.
7. FitzGerald JJ, Rosendal F, de Pennington N, et al. Long-term outcome of deep brain stimulation in generalised dystonia: A series of 60 cases. *J Neurol Neurosurg Psychiatry.* 2014;85(12):1371–1376.
8. Behrens TEJ, Johansen-Berg H, Woolrich MW, et al. Non-invasive mapping of connections between human thalamus and cortex using diffusion imaging. *Nat Neurosci.* 2003;6(7):750–757.
9. Schönecker T, Gruber D, Kivi A, et al. Postoperative MRI localisation of electrodes and clinical efficacy of pallidal deep brain stimulation in cervical dystonia. *J Neurol Neurosurg Psychiatry.* 2015;86(8):833–839.
10. Neumann W, Horn A, Ewert S, et al. A localized pallidal physiomarker in cervical dystonia. *Ann Neurol.* 2017;82(6):912–924.
11. Tziortzi AC, Haber SN, Searle GE, et al. Connectivity-based functional analysis of dopamine release in the striatum using diffusion-weighted MRI and positron emission tomography. *Cereb Cortex.* 2014;24(5):1165–1177.
12. Patriat R, Cooper SE, Duchin Y, et al. Individualized tractography-based parcellation of the globus pallidus pars interna using 7T MRI in movement disorder patients prior to DBS surgery. *Neuroimage.* 2018;178:198–209.
13. Colosimo C, Pantano P, Calistri V, Totaro P, Fabbrini G, Berardelli A. Diffusion tensor imaging in primary cervical dystonia. *J Neurol Neurosurg Psychiatry.* 2005;76(11):1591–1593.
14. Delmaire C, Krainik A, Tézenas Du Montcel S, et al. Disorganized somatotopy in the putamen of patients with focal hand dystonia. *Neurology.* 2005;64(8):1391–1396.
15. Moore RD, Gallea C, Horovitz SG, Hallett M. Individuated finger control in focal hand dystonia: An fMRI study. *Neuroimage.* 2012;61(4):823–831.
16. Delnooz CCS, Pasman JW, Beckmann CF, van de Warrenburg BPC. Altered striatal and pallidal connectivity in cervical dystonia. *Brain Struct Funct.* 2015;220(1):513–523.
17. Antoniades CA, Rebelo P, Kennard C, Aziz TZ, Green AL, FitzGerald JJ. Pallidal deep brain stimulation improves higher control of the oculomotor system in Parkinson's disease. *J Neurosci.* 2015;35(38):13043–13052.
18. Lenz FA, Byl NN. Reorganization in the cutaneous core of the human thalamic principal somatic sensory nucleus (ventral caudal) in patients with dystonia. *J Neurophysiol.* 1999;82(6):3204–3212.
19. Ridding MC, Sheean G, Rothwell JC, Inzelberg R, Kujirai T. Changes in the balance between motor cortical excitation and

- inhibition in focal, task specific dystonia. *J Neurol Neurosurg Psychiatry*. 1995;59(5):493–498.
20. Garibotto V, Romito LM, Elia AE, et al. In vivo evidence for GABA_A receptor changes in the sensorimotor system in primary dystonia: GABA_A Receptor Changes in Primary Dystonia. *Mov Disord*. 2011;26(5):852–857.
 21. Edwards MJ, Huang Y-Z, Mir P, Rothwell JC, Bhatia KP. Abnormalities in motor cortical plasticity differentiate manifesting and nonmanifesting DYT1 carriers. *Mov Disord*. 2006;21(12):2181–2186.
 22. Quartarone A, Rizzo V, Terranova C, et al. Abnormal sensorimotor plasticity in organic but not in psychogenic dystonia. *Brain*. 2009;132(Pt 10):2871–2877.
 23. Weise D, Schramm A, Stefan K, et al. The two sides of associative plasticity in writer's cramp. *Brain*. 2006;129(Pt 10):2709–2721.
 24. Richardson SP. Enhanced dorsal premotor–motor inhibition in cervical dystonia. *Clin Neurophysiol*. 2015;126:1387–1391.
 25. Sadnicka A, Kimmich O, Pisarek C, et al. Pallidal stimulation for cervical dystonia does not correct abnormal temporal discrimination: GPI-DBS for CD does not correct abnormal TDT. *Mov Disord*. 2013;28(13):1874–1877.
 26. Tang JKH, Mahant N, Cunic D, et al. Changes in cortical and pallidal oscillatory activity during the execution of a sensory trick in patients with cervical dystonia. *Exp Neurol*. 2007;204(2):845–848.
 27. Ni Z, Kim SJ, Phielipp N, et al. Pallidal deep brain stimulation modulates cortical excitability and plasticity: Pallidal DBS. *Ann Neurol*. 2018;83(2):352–362.
 28. Kuhn AA, Meyer B-U, Trottenberg T, Brandt SA, Schneider GH, Kupsch A. Modulation of motor cortex excitability by pallidal stimulation in patients with severe dystonia. *Neurology*. 2003;60(5):768–774.
 29. Tisch S, Rothwell JC, Bhatia KP, et al. Pallidal stimulation modifies after-effects of paired associative stimulation on motor cortex excitability in primary generalised dystonia. *Exp Neurol*. 2007;206(1):80–85.
 30. Detante O, Vercueil L, Thobois S, et al. Globus pallidus internus stimulation in primary generalized dystonia: A H215O PET study. *Brain*. 2004;127(Pt 8):1899–1908.
 31. Horn A, Li N, Dembek TA, et al. Lead-DBS v2: Towards a comprehensive pipeline for deep brain stimulation imaging. *Neuroimage*. 2019;184:293–316.